

412 **DISCUSSION**

413         The importance of satellite cell proliferation activity in skeletal muscle repair and  
414 hypertrophy has been appreciated for a considerable time. It is well documented that one  
415 of the earliest events, triggering the activation of quiescent satellite cells, is initiated by  
416 mechanical or chemical stimuli and enables satellite cells to migrate and enter the cell  
417 proliferation cycle. Bischoff (11) was among the first to explore the biochemical link  
418 between satellite cell activation and mechanical perturbation of muscle tissue. His  
419 classical experiments used a crushed-muscle extract, which he found could stimulate  
420 satellite cells associated with isolated fibers to synthesize DNA and divide. Johnson and  
421 Allen (30) later reported that the same crushed-muscle extract could stimulate adult rat  
422 satellite cells in culture to enter the cell cycle earlier than adult rat cultures in control  
423 medium. Shortening of the lag phase observed with freshly isolated adult satellite cells  
424 has since been used as an assay for satellite cell activation (1, 2, 58) and this assay was  
425 employed in experiments that first demonstrated that HGF was unique in its ability to  
426 activate satellite cell division in vitro (1). In subsequent experiments, the active agent in  
427 crushed-muscle extract was shown to be HGF, which was present in un-injured muscle and  
428 located primarily in the extracellular matrix (58, 62). In further experiments, Tatsumi et al.  
429 (59-61, 64) showed that satellite cells were stimulated to enter the cell cycle when subjected  
430 to mechanical stretch in primary culture and living muscle. We also demonstrated that  
431 satellite cell activation was due to rapid release of HGF from its extracellular tethering and  
432 the subsequent presentation to the receptor c-met, and later verified that HGF release is  
433 dependent on calcium-calmodulin formation and the down-stream NO radical-mediated  
434 activation of matrix metalloproteinases (MMPs) (47, 67, 75, 76).

435         These observations suggest that the stretch-activation of satellite cells is a cascade of  
436 sequential events including (in order) an influx of calcium ions and their binding to  
437 calmodulin, NO radical production by cNOS, MMP activation, HGF release from the matrix  
438 and presentation of HGF to the signaling receptor c-met (see a review of Ref. 66). In this  
439 model, a complex of HGF and proteoglycan extracellular domain would be shed from the  
440 matrix and presented to the receptor c-met. In fact, HGF associated with heparan sulfate  
441 moieties has a greater affinity for c-met relative to HGF alone, and therefore, has enhanced  
442 HGF signaling activity (20). Such a complex has been detected in PBS extracts from  
443 crushed muscle and intact muscle incubated in the NO donor, sodium nitroprusside (SNP)  
444 (Allen et al., unpublished data), supporting the above insight. In related experiments by

445 Wozniak and Anderson (73), released HGF may induce c-met expression as an  
446 immediate-early gene, thus also enhance HGF-c-met signaling in the satellite cell activation  
447 process. They additionally observed that the level of satellite cell activation was increased  
448 in un-stretched fibers from mdx and nNOS-knockout mice and in un-stretched normal fibers  
449 by treatment with a competitive NOS-inhibitor L-NAME (N<sup>G</sup>-nitro-L-arginine methylester),  
450 suggesting that a NO-independent HGF/c-met signaling pathway, and possibly other  
451 signaling pathways, control activation in muscle deficient in dystrophin and nNOS (73).

452 It has not been determined how quiescent satellite cells sense mechanical stimuli to  
453 generate biochemical signals that elevate intracellular calcium ion concentrations; therefore,  
454 in the present work, the involvement of MS- and VGC-channels in the  
455 mechano-transduction system was examined. When satellite cell cultures were incubated  
456 with the MS-channel inhibitor GsMTx-4, the L-VGC-channel inhibitor nifedipine, or a less  
457 specific inhibitor, gadolinium chloride, stretch-induced HGF release from the matrix and the  
458 resulting cell activation were abolished completely in a dose-dependent manner. This was  
459 revealed by western blotting of conditioned media and a BrdU-incorporation assay (Fig. 2).  
460 By contrast, the T-VGC-channel inhibitor NNC55-0396 did not have inhibitory effects on  
461 the activation index. Addition of the calcium-chelator EGTA to culture media also  
462 inhibited the stretch-activation response and HGF release, indicating the significance of  
463 extracellular calcium ions in the activation cascade (Fig. 1 and Fig. 2 panel B). This  
464 means that free calcium ions stored in mitochondria may now be excluded from a role in  
465 this activation pathway. Calcium-imaging analyses verified these results, and therefore  
466 provide direct evidence that both MS- and L-VGC-channels are essential in calcium ion  
467 influx in response to mechanical stretch and that calcium ions may flow in through  
468 L-VGC-channels (Fig. 4). A possible explanation for these observations can be addressed  
469 by a possible model of MS-/L-VGC-channel coupling, in which the MS-channel responds  
470 to mechanical stimuli by gating cations; this would result in local depolarization of the  
471 plasma membrane, a signal that is then quickly sensed by L-VGC-channels (Ca<sub>v1.1</sub>, Ca<sub>v1.2</sub>)  
472 that allow a significant amount of calcium ions to permeate the cell and lead to  
473 calcium-calmodulin formation (see Fig. 5 panel B for details). In the nifedipine treatment,  
474 in which MS-channels are expected to retain biological activity to gate selective cations,  
475 significant calcium influx was not observed, suggesting that MS-channels concerned in the  
476 activation pathway allow entry of cations other than calcium ions and/or gate an  
477 undetectable level of calcium ions that is not sufficient to activate calmodulin-NOS

478 signaling directly but is enough to depolarize the cell membrane.

479         Considering the possible implication of MS-channels in the mechano-sensing  
480 mechanism of satellite cell activation, it is worth noting the valuable study by Formigli et al.  
481 (25), which provided the first experimental evidence that the transient receptor potential  
482 canonical channel 1 (TRPC1) represents an essential component of stretch-activated cation  
483 channel signaling in the mouse C2C12 myoblast cell line, as assayed by whole-cell  
484 patch-clamp and atomic force microscopic pulling. That study indicated that TRPC1 plays  
485 a crucial role in mechano-transduction during regulation of the early phases of myoblast  
486 differentiation. TRPCs (TRPC1-7) are a family of cation channels that assemble as homo-  
487 or hetero-tetramers to form voltage-independent, non-selective cation- ( $\text{Na}^+$  and  $\text{Ca}^{2+}$ )  
488 permeable pores (16, 46). Although numerous studies have shown that TRPC1 may be  
489 store-operated calcium-ion entry channels (SOCs) in various cell types (23, 74), there is  
490 also evidence that this channel is able to translate membrane stretch into cation currents  
491 across the plasma membrane (17, 37, 52). TRPC5 and 6 were also shown to be  
492 stretch-gated and GsMTx-4-sensitive cation-channels and TRPC6 plays an essential role of  
493 mechano-sensing in smooth muscle cells (26, 51; reviewed in Ref. 13), therefore, at least at  
494 this time, TRPC1, 5, and 6 may be reasonable candidates for the MS-channel in the satellite  
495 cell activation pathway concerned here. Our rat satellite cell cultures expressed TRPC1  
496 message, as revealed by RT-PCR, while TRPC6 was not detected at 24-hr post-plating (Fig.  
497 3 panel B), which is the time-point at which the stretch treatment was applied in the present  
498 and our previous experiments (65, 75-77); this provides a supportive background for the  
499 implication of TRPC1 in the above model of stretch-activation. TRPA1 (18), TRPV4 (10)  
500 and TRPM7 (41) are also reported to be stretch-sensitive channels and therefore can not be  
501 excluded from the list of candidate MS-channels at the present time, and the field awaits a  
502 study to examine their GsMTx-4 sensitivity and expression in quiescent satellite cells.

503         Another important observation by Formigli et al. (25) is that TRPC1 activity and  
504 stretch-induced cation influx in C2C12 myoblasts were modulated by  
505 sphingosine-1-phosphate (S1P), an important bioactive sphingolipid-metabolite that mainly  
506 acts through G-protein-coupled receptors present on mammalian cells, and thereby regulates  
507 numerous cell functions including cell proliferation, differentiation and apoptosis (78). In  
508 line with this, TRPC1 expression is reported to be significantly up-regulated during  
509 myogenesis, especially in the presence of S1P, supporting the physiological relevance of the  
510 sphingosine-S1P-TRPC1 axis in regulating C2C12 cell growth and differentiation (24, 25,

511 39). Notably, Nagata et al. (40) clearly showed that S1P can induce satellite cells to enter  
512 the cell cycle, whereas inhibiting the sphingolipid signaling cascade (which generates S1P  
513 mainly from sphingomyelin and sphingosine by N-SMase, ceramidase and sphingosine  
514 kinase) reduces the number of satellite cells able to divide in response to mitogen  
515 stimulation. A similar observation was reported by Sassoli et al. (48); S1P promotes  
516 satellite cell renewal and differentiation in damaged muscle. Although the S1P-mediated  
517 activation pathway is not well elucidated at the present time, considering the regulative role  
518 of S1P in TRPC1 gating in C2C12 myoblasts (25), one possible hypothesis may be that S1P  
519 associates with TRPC1 (and/or TRPC5, 6) directly or indirectly and can trigger satellite cell  
520 activation even without stretch stimuli. Alternatively, S1P could drastically decrease the  
521 threshold intensity of stretch that is required for TRPC gating; this would be followed by  
522 L-VGC-channel activation and lead to influx of extracellular calcium ions and their  
523 subsequent presentation to calmodulin to form calcium-calmodulin complexes as the cNOS  
524 activator. In line with this, it is worth noting the excellent study by Sbrana et al. (49),  
525 which showed that S1P activates the cytoskeleton contraction that in turn stretches the cell  
526 membrane and increases its stiffness; therefore such changes may improve the  
527 mechano-sensitivity of un-stretched C2C12 myoblasts. This S1P-TRPC scenario was  
528 recently addressed by some focused studies on TRPC functions related to sphingolipid  
529 biology, and therefore does not exclude other possibilities including that the S1P pathway is  
530 not dependent on either TRPC signaling or the activation cascade concerned here.

531 In summary, the present experiments bridge the gap between mechanical stretch  
532 stimuli and the increase in intracellular calcium-ion concentration by demonstrating that  
533 inhibition of MS-channels and L-VGC-channels in vitro, prior to mechanical stretch,  
534 prevents the influx of extracellular calcium ions, HGF-release from the matrix and re-entry  
535 of adult satellite cells into the cell cycle. The physiological significance of the  
536 MS-channel gating-initiated pathway described using cultured satellite cells remains to be  
537 verified in muscle fibers, as does the crucial role of calcium-calmodulin formation in the  
538 NO-radical production by cNOS that was described recently in isolated satellite cells in  
539 culture (67). Nonetheless, the current report demonstrated that in isolated satellite cells, a  
540 functional coupling of MS-channel and L-VGC-channel gating plays the central role in  
541 mechano-sensing machinery that instigates the activation of satellite cells.

542

543

544 **ACKNOWLEDGMENTS**

545 We are grateful to T. Tamura of Nikon Instech for technical assistance with the  
546 calcium imaging. The G3G4 mouse anti-BrdU monoclonal antibody developed by S. J.  
547 Kaufman and D3 anti-desmin monoclonal antibody developed by D. A. Fischman were  
548 obtained from the Developmental Studies Hybridoma Bank, developed under the auspices  
549 of the NICHD and maintained by The University of Iowa, Department of Biological  
550 Sciences, Iowa City, IA 52242, Iowa.

551

552

553 **GRANTS**

554 This work was supported by Grants-in-Aid for Scientific Research (B) 19380152 and  
555 22380145 from the Japan Society for the Promotion of Science (JSPS) (all to R. Tatsumi)  
556 and by a research grant of the Graduate School Student Projects Academic Challenge 2010  
557 from the Entrepreneurship Center of Kyushu University (to M. Hara). The research was  
558 also supported by funds from the Arizona Agriculture Experiment Station and grants from  
559 the US Department of Agriculture National Research Initiative Competitive Grant  
560 2005-35206-15255 and Muscular Dystrophy Association Grant MDA3685 (all to R. E.  
561 Allen), and by funds from the Canadian Space Agency 9F007-52237-001-SR and the  
562 Natural Sciences and Engineering Research Council 171302 (to J. E. Anderson). M.-K. Q.  
563 Do received a scholarship from the Ministry of Education, Culture, Sports, Science and  
564 Technology-Japan (MEXT) during the course of this research.

565

566

567

## 568 REFERENCES

- 569 1. **Allen RE, Sheehan SM, Tayler RG, Kendall TL, Rice GM.** Hepatocyte growth  
570 factor activates quiescent skeletal muscle satellite cells in vitro. *J Cell Physiol* 165:  
571 307–312, 1995.
- 572 2. **Allen RE, Temm-Grove CJ, Sheehan SM, Rice GM.** Skeletal muscle satellite cell  
573 cultures. *Methods Cell Biol* 52: 155-176, 1997.
- 574 3. **Andersen OS, Koeppe II RE.** Bilayer thickness and membrane protein function: an  
575 energetic perspective. *Annu Rev Biophys Biomol Struct* 36: 107-130, 2007.
- 576 4. **Anderson JE.** A role for nitric oxide in muscle repair: nitric oxide-mediated  
577 activation of muscle satellite cells. *Mol Biol Cell* 11: 1859-1874, 2000.
- 578 5. **Anderson JE, Pilipowicz O.** Activation of muscle satellite cells in single-fiber  
579 cultures. *Nitric Oxide* 7: 36-41, 2002.
- 580 6. **Anderson JE, Vargas C.** Correlated NOS-Im $\mu$  and myf5 expression by satellite  
581 cells in mdx mouse muscle regeneration during NOS manipulation and deflazacort  
582 treatment. *Neuromuscul Disord* 13: 388-396, 2003.
- 583 7. **Anderson JE, Wozniak AC.** Satellite cell activation on fibers: modeling events in  
584 vivo. *Can J Physiol Pharmacol* 82: 300-310, 2004.
- 585 8. **Anderson JE.** The satellite cell as a companion in skeletal muscle plasticity:  
586 currency, conveyance, clue, connector and colander. *J Exp Biol* 209: 2276-2292,  
587 2006.
- 588 9. **Árnadóttir J, Chalfie M.** Eukaryotic mechanosensitive channels. *Annu Rev*  
589 *Biophys* 39: 111-137, 2010.
- 590 10. **Becker D, Blase C, Bereiter-Hahn J, Jendrach M.** TRPV4 exhibits a functional role  
591 in cell-volume regulation. *J Cell Sci* 118: 2435-2440, 2005.
- 592 11. **Bischoff R.** A satellite cell mitogen from crushed adult muscle. *Dev Biol* 115:  
593 140-147, 1986.
- 594 12. **Bischoff R.** The satellite cell and muscle regeneration. In: *Myology: Basic and*  
595 *Clinical*, 2nd ed., edited by Engel AG and Franzini-Armstrong C. New York:  
596 McGraw-Hill, 1994, vol. 1, p. 97-118.
- 597 13. **Bowman CL, Gottlieb PA, Suchyna TM, Murphy YK, Sachs F.**  
598 Mechanosensitive ion channels and the peptide inhibitor GsMTx-4: history, properties,  
599 mechanisms and pharmacology. *Toxicon* 49: 249-270, 2007.
- 600 14. **Catterall WA.** Signaling complexes of voltage-gated sodium and calcium channels.  
601 *Neurosci Lett* 486: 107-116, 2010.
- 602 15. **Chargé SB, Rudnicki MA.** Cellular and molecular regulation of muscle  
603 regeneration. *Physiol Rev* 84: 209-238, 2004.
- 604 16. **Clapham DE.** TRP channels as cellular sensors. *Nature* 426: 517-524, 2003.
- 605 17. **Clark K, Middelbeek J, van Leeuwen FN.** Interplay between TRP channels and  
606 the cytoskeleton in health and disease. *Eur J Cell Biol* 87: 631-640, 2008.
- 607 18. **Corey DP, García-Añoveros J, Holt JR, Kwan KY, Lin SY, Vollrath MA,**  
608 **Amalfitano A, Cheung EL, Derfler BH, Duggan A, Géléoc GS, Gray PA, Hoffman**  
609 **MP, Rehm HL, Tamasauskas D, Zhang DS.** TRPA1 is a candidate for the  
610 mechanosensitive transduction channel of vertebrate hair cells. *Nature* 432: 723-730,  
611 2004.
- 612 19. **Cornelison DDW, Wold BJ.** Single-cell analysis of regulatory gene expression in  
613 quiescent and activated mouse skeletal muscle satellite cells. *Dev Biol* 191: 270-283,  
614 1997.

- 615 20. **Derksen PW, Keehnen RM, Evers LM, van Oers MH, Spaargaren M, Pals ST.**  
616 Cell surface proteoglycan syndecan-1 mediates hepatocyte growth factor binding and  
617 promotes Met signaling in multiple myeloma. *Blood* 99: 1405-1410, 2002.
- 618 21. **Dulhunty AF.** Excitation-contraction coupling from the 1950s into the new  
619 millennium. *Clin Exp Pharmacol Physiol* 33: 763-772, 2006.
- 620 22. **Engelman DM.** Membranes are more mosaic than fluid. *Nature* 438: 578-580,  
621 2005.
- 622 23. **Fiorio Pla A, Maric D, Brazer SC, Giacobini P, Liu X, Chang YM, Ambudkar IS,**  
623 **Barker JL.** Canonical transient receptor potential 1 plays a role in basic fibroblast  
624 growth factor (bFGF)/FGF receptor-1-induced  $Ca^{2+}$  entry and embryonic rat neural  
625 stem cell proliferation. *J Neurosci* 25: 2687-2701, 2005.
- 626 24. **Formigli L, Meacci E, Sassoli C, Squecco R, Nosi D, Chellini F, Naro F, Francini**  
627 **F, Zecchi-Orlandini S.** Cytoskeleton/stretch-activated ion channel interaction  
628 regulates myogenic differentiation of skeletal myoblasts. *J Cell Physiol* 211:  
629 296-306, 2007.
- 630 25. **Formigli L, Sassoli C, Squecco R, Bini F, Martinesi M, Chellini F, Luciani G,**  
631 **Sbrana F, Zecchi-Orlandini S, Francini F, Meacci E.** Regulation of transient  
632 receptor potential canonical channel 1 (TRPC1) by sphingosine 1-phosphate in C2C12  
633 myoblasts and its relevance for a role of mechanotransduction in skeletal muscle  
634 differentiation. *J Cell Sci* 122: 1322-1333, 2009.
- 635 26. **Gomis A, Soriano S, Belmonte C, Viana, F'.** Hypoosmotic- and pressure-induced  
636 membrane stretch activate TRPC5 channels. *J Physiol* 586: 5633-5649, 2008.
- 637 27. **Haswell ES, Phillips R, Rees DC.** Mechanosensitive channels: what can they do  
638 and how do they do it? *Structure* 19: 1356-1369, 2011.
- 639 28. **Hawke TJ, Garry DJ.** Myogenic satellite cells: physiology to molecular biology.  
640 *J Appl Physiol* 91: 534-551, 2001.
- 641 29. **Huang L, Keyser BM, Tagmose TM, Hansen JB, Taylor JT, Zhuang H, Zhang M,**  
642 **Ragsdale DS, Li M.** NNC 55-0396  
643 [(1S,2S)-2-(2-(N-[(3-benzimidazol-2-yl)propyl]-N-methylamino)ethyl)-6-fluoro-1,2,3,  
644 4-tetrahydro-1-isopropyl-2-naphthyl cyclopropanecarboxylate dihydrochloride]: a new  
645 selective inhibitor of T-type calcium channels. *J Pharmacol Exp Ther* 309: 193-199,  
646 2004.
- 647 30. **Johnson SE, Allen RE.** Proliferating cell nuclear antigen (PCNA) is expressed in  
648 activated rat skeletal muscle satellite cells. *J Cell Physiol* 154: 39-43, 1993.
- 649 31. **Kobayashi T, Sokabe M.** Sensing substrate rigidity by mechanosensitive ion  
650 channels with stress fibers and focal adhesions. *Curr Opin Cell Biol* 22: 669-676,  
651 2010.
- 652 32. **Kuang S, Gillespie MA, Rudnicki MA.** Niche regulation of muscle satellite cell  
653 self-renewal and differentiation. *Cell Stem Cell* 2: 22-31, 2008.
- 654 33. **Kung C, Martinac B, Sukharev S.** Mechanosensitive channels in microbes. *Annu*  
655 *Rev Microbiol* 64: 313-329, 2010.
- 656 34. **Lacinová L.** Voltage-dependent calcium channels. *Gen Physiol Biophys* 24: 1-78,  
657 2005.
- 658 35. **Laemmli UK.** Cleavage of structural proteins during the assembly of the head of  
659 bacteriophage T4. *Nature* 277: 680-685, 1970.
- 660 36. **Lipscombe D, Helton TD, Xu W.** L-type calcium channels: the low down. *J*  
661 *Neurophysiol* 92: 2633-2641, 2004.

- 662 37. **Maroto R, Raso A, Wood TG, Kurosky A, Martinac B, Hamill OP.** TRPC1 forms  
663 the stretch-activated cation channel in vertebrate cells. *Nature Cell Biol* 7: 179-185,  
664 2005.
- 665 38. **Martins KJB, Maclean I, Murdoch GK, Dixon WT, Putman CT.** Nitric oxide  
666 synthase inhibition delays low frequency stimulation-induced satellite cell activation  
667 in rat fast-twitch muscle. *Appl Physiol Nutr Metab* 36: 996-1000, 2011.
- 668 39. **Meacci E, Nuti F, Donati C, Cencetti F, Farnararo M, Bruni P.** Sphingosine  
669 kinase activity is required for myogenic differentiation of C2C12 myoblasts. *J Cell*  
670 *Physiol* 214: 210-220, 2008.
- 671 40. **Nagata Y, Partridge TA, Matsuda R, Zammit PS.** Entry of muscle satellite cells  
672 into the cell cycle requires sphingolipid signaling. *J Cell Biol* 174: 245-253, 2006.
- 673 41. **Numata T, Shimizu T, Okada Y.** TRPM7 is a stretch- and swelling-activated cation  
674 channel involved in volume regulation in human epithelial cells. *Am J Physiol Cell*  
675 *Physiol* 292: C460-C467, 2007.
- 676 42. **Perozo E, Cortes DM, Sompornpisut P, Kloda A, Martinac B.** Open channel  
677 structure of MscL and the gating mechanism of mechanosensitive channels. *Nature*  
678 418: 942-948, 2002.
- 679 43. **Persechini A, McMillan K, Leakey P.** Activation of myosin light chain kinase and  
680 nitric oxide synthase activities by calmodulin fragments. *J Biol Chem* 269:  
681 16148-16154, 1994.
- 682 44. **Rios E, Brum G.** Involvement of dihydropyridine receptors in  
683 excitation-contraction coupling in skeletal muscle. *Nature* 325: 717-720, 1987.
- 684 45. **Roel W ten Broek, Grefte S, Johannes W Von den Hoff.** Regulatory factors and  
685 cell populations involved in skeletal muscle regeneration. *J Cell Physiol* 224: 7-16,  
686 2010.
- 687 46. **Rychkov G, Barritt GJ.** TRPC1 Ca<sup>2+</sup>-permeable channels in animal cells. *Handb*  
688 *Exp Pharmacol* 179: 23-52, 2007.
- 689 47. **Sakata T, Tatsumi R, Yamada M, Shiratsuchi S, Okamoto S, Mizunoya W,**  
690 **Hattori A, Ikeuchi Y.** Preliminary experiments on mechanical stretch-induced  
691 activation of skeletal muscle satellite cells in vivo. *Anim Sci J* 77: 518-525, 2006.
- 692 48. **Sassoli C, Formigli L, Bini F, Tani A, Squecco R, Battistini C, Zecchi-Orlandini S,**  
693 **Francini F, Meacci E.** Effects of S1P on skeletal muscle repair/regeneration during  
694 eccentric contraction. *J Cell Mol Med* 15: 2498-2511, 2011.
- 695 49. **Sbrana F, Sassoli C, Meacci E, Nosi D, Squecco R, Paternostro F, Tiribilli B,**  
696 **Zecchi-Orlandini S, Francini F, Formigli L.** Role for stress fiber contraction in  
697 surface tension development and stretch-activated channel regulation in C2C12  
698 myoblasts. *Am J Physiol Cell Physiol* 295: C160-C172, 2008.
- 699 50. **Seale P, Rudnicki MA.** A new look at the origin, function, and “Stem-Cell” status  
700 of muscle satellite cells. *Dev Biol* 218: 115-124, 2000.
- 701 51. **Spasova MA, Hewavitharana T, Xu W, Soboloff J, Gill DL.** A common  
702 mechanism underlies stretch activation and receptor activation of TRPC6 channels.  
703 *Proc Natl Acad Sci USA* 103: 16586-16591, 2006.
- 704 52. **Stiber JA, Zhang ZS, Burch J, Eu JP, Zhang S, Truskey GA, Seth M, Yamaguchi**  
705 **N, Meissner G, Shah R, Worley PF, Williams RS, Rosenberg PB.** Mice lacking  
706 Homer 1 exhibit a skeletal myopathy characterized by abnormal transient receptor  
707 potential channel activity. *Mol Cell Biol* 28: 2637-2647, 2008.



- 708 53. **Striessnig J.** Ca<sup>2+</sup> channel blockers. In: *Encyclopedic reference of molecular*  
709 *pharmacology*, edited by Offermanns S and Rosenthal W. Berlin: Springer, 2004, p.  
710 201-207.
- 711 54. **Suchyna TM, Tape SE, Koeppe RE II, Andersen OS, Sachs F, Gottlieb PA.**  
712 Bilayer-dependent inhibition of mechanosensitive channels by neuroactive peptide  
713 enantiomers. *Nature* 430: 235-240, 2004.
- 714 55. **Tai CH, Yang YC, Pan MK, Huang CS, Kuo CC.** Modulation of subthalamic  
715 T-type Ca<sup>2+</sup> channels remedies locomotor deficits in a rat model of Parkinson disease.  
716 *J Clin Invest* 121: 3289-3305, 2011.
- 717 56. **Takenaka T, Suzuki H, Okada H, Hayashi K, Ozawa Y, Saruta T.** Biophysical  
718 signals underlying myogenic responses in rat interlobular artery. *Hypertension* 32:  
719 1060-1065, 1998a.
- 720 57. **Takenaka T, Suzuki H, Okada H, Hayashi K, Kanno Y, Saruta T.**  
721 Mechanosensitive cation channels mediate afferent arteriolar myogenic constriction in  
722 the isolated rat kidney. *J Physiol* 511: 245-253, 1998b.
- 723 58. **Tatsumi R, Anderson JE, Nevoret CJ, Halevy O, Allen RE.** HGF/SF is present in  
724 normal adult skeletal muscle and is capable of activating satellite cells. *Dev Biol*  
725 194: 114-128, 1998.
- 726 59. **Tatsumi R, Sheehan SM, Iwasaki H, Hattori A, Allen RE.** Mechanical stretch  
727 induces activation of skeletal muscle satellite cells in vitro. *Exp Cell Res* 267:  
728 107-114, 2001.
- 729 60. **Tatsumi R, Hattori A, Ikeuchi Y, Anderson JE, Allen RE.** Release of hepatocyte  
730 growth factor from mechanically stretched skeletal muscle satellite cells and role of  
731 pH and nitric oxide. *Mol Biol Cell* 13: 2909-2918, 2002a.
- 732 61. **Tatsumi R, Hattori A, Allen RE, Ikeuchi Y, Ito T.** Mechanical stretch-induced  
733 activation of skeletal muscle satellite cells is dependent on nitric oxide production in  
734 vitro. *Anim Sci J* 73: 235-239, 2002b.
- 735 62. **Tatsumi R, Allen RE.** Active hepatocyte growth factor is present in skeletal muscle  
736 extracellular matrix. *Muscle Nerve* 30: 654-658, 2004.
- 737 63. **Tatsumi R, Mitsuhashi K, Ashida K, Haruno A, Hattori A, Ikeuchi Y, Allen RE.**  
738 Comparative analysis of mechanical stretch-induced activation activity of back and leg  
739 muscle satellite cells in vitro. *Anim Sci J* 75: 345-351, 2004.
- 740 64. **Tatsumi R, Liu X, Pulido A, Morales M, Sakata T, Dail S, Hattori A, Ikeuchi Y,**  
741 **Allen RE.** Satellite cell activation in stretched skeletal muscle and the role of nitric  
742 oxide and hepatocyte growth factor. *Am J Physiol Cell Physiol* 290: C1487-C1494,  
743 2006a.
- 744 65. **Tatsumi R, Yamada M, Katsuki Y, Okamoto S, Ishizaki J, Mizunoya W, Ikeuchi**  
745 **Y, Hattori A, Shimokawa H, Allen RE.** Low-pH preparation of skeletal muscle  
746 satellite cells can be used to study activation in vitro. *Int J Biochem Cell Biol* 38:  
747 1678-1685, 2006b.
- 748 66. **Tatsumi R, Allen RE.** Mechano-biology of resident myogenic stem cells: molecular  
749 mechanism of stretch-induced activation of satellite cells. *Anim Sci J* 79: 279-290,  
750 2008.
- 751 67. **Tatsumi R, Wuollet AL, Tabata K, Nishimura S, Tabata S, Mizunoya W, Ikeuchi**  
752 **Y, Allen RE.** A role for calcium-calmodulin in regulating nitric oxide production  
753 during skeletal muscle satellite cell activation. *Am J Physiol Cell Physiol* 296:  
754 C922-C929, 2009.

- 755 68. **Tatsumi R.** Mechano-biology of skeletal muscle hypertrophy and regeneration:  
756 possible mechanism of stretch-induced activation of resident myogenic stem cells.  
757 *Anim Sci J* 81: 11-20, 2010.
- 758 69. **Weissman BA, Jones CL, Liu Q, Gross SS.** Activation and inactivation of  
759 neuronal nitric oxide synthase: characterization of Ca<sup>2+</sup>-dependent [<sup>125</sup>I]calmodulin  
760 binding. *Eur J Pharmacol* 435: 9-18, 2002.
- 761 70. **Welsh DG, Morielli AD, Nelson MT, Brayden JE.** Transient receptor potential  
762 channels regulate myogenic tone of resistance arteries. *Circ Res* 90: 248-250, 2002.
- 763 71. **Wozniak AC, Pilipowicz O, Yablonka-Reuveni Z, Greenway S, Craven S, Scott E,**  
764 **Anderson JE.** C-met expression and mechanical activation of satellite cells on  
765 cultured muscle fibers. *J Histochem Cytochem* 51: 1-9, 2003.
- 766 72. **Wozniak AC, Kong J, Bock E, Pilipowicz O, Anderson JE.** Signaling satellite-cell  
767 activation in skeletal muscle: markers, models, stretch, and potential alternate  
768 pathways. *Muscle Nerve* 31: 283-300, 2005.
- 769 73. **Wozniak AC, Anderson JE.** Nitric oxide-dependence of satellite stem cell  
770 activation and quiescence on normal skeletal muscle fibers. *Dev Dyn* 236: 240-250,  
771 2007.
- 772 74. **Wu X, Zagranichnaya TK, Gurda GT, Eves EM, Villereal ML.** A  
773 TRPC1/TRPC3-mediated increase in store-operated calcium entry is required for  
774 differentiation of H19-7 hippocampal neuronal cells. *J Biol Chem* 279: 43392-43402,  
775 2004.
- 776 75. **Yamada M, Tatsumi R, Kikuri T, Okamoto S, Nonoshita S, Mizunoya W, Ikeuchi**  
777 **Y, Shimokawa H, Sunagawa K, Allen RE.** Matrix metalloproteinases are involved  
778 in mechanical stretch-induced activation of skeletal muscle satellite cells. *Muscle*  
779 *Nerve* 34: 313-319, 2006.
- 780 76. **Yamada M, Sankoda Y, Tatsumi R, Mizunoya W, Ikeuchi Y, Sunagawa K, Allen**  
781 **RE.** Matrix metalloproteinase-2 mediates stretch-induced activation of skeletal  
782 muscle satellite cells in a nitric oxide dependent manner. *Int J Biochem Cell Biol* 40:  
783 2183-2191, 2008.
- 784 77. **Yamada M, Tatsumi R, Yamanouchi K, Hosoyama T, Shiratsuchi S, Sato A,**  
785 **Ikeuchi Y, Furuse M, Allen RE.** High concentrations of HGF inhibit skeletal  
786 muscle satellite cell proliferation in vitro by inducing expression of myostatin: a  
787 possible mechanism for reestablishing satellite cell quiescence in vivo. *Am J Physiol*  
788 *Cell Physiol* 298: C465-C476, 2010.
- 789 78. **Zeidan YH, Hannun YA.** Translational aspects of sphingolipid metabolism.  
790 *Trends Mol Med* 13: 327-336, 2007.  
791  
792  
793

794 **FIGURE LEGENDS**

795 Fig. 1. Significance of extracellular calcium ions in stretch-activation of satellite cells in  
 796 vitro. Satellite cells from adult rat skeletal muscle were stretched in culture (*black bars*)  
 797 for 1 hr beginning at 24-hr post-plating in FlexerCell FX-2000 System (25% stretch at  
 798 12-sec intervals, as originally optimized in Tatsumi et al. (59) and shown in panel *A* again)  
 799 in the presence (*bar d*) or absence (*bar c*) of 1.8 mM ethyleneglycol tetraacetic acid (EGTA)  
 800 in DMEM-10% normal horse serum (pH 7.2), followed an assay to detect activation using  
 801 bromodeoxyuridine (BrdU) at 48-hr post-plating. This experiment also included the  
 802 following control cultures: *bar a*, un-stretched culture; *bar b*, 2-hr stretch culture  
 803 (equivalent to our regular period of stretch, originally described in Ref. 59); *bar e*, stretched  
 804 culture receiving 1.8 mM EGTA for 24-48 hr post-plating; *bar f*, positive control culture  
 805 supplemented with 2.5 ng/ml recombinant mouse hepatocyte growth factor (HGF) for 24-48  
 806 hr; *bar g*, HGF culture receiving 1.8 mM EGTA for 24-48 hr; *bars h* and *i*, control cultures  
 807 with 1.8 mM EGTA for 24-25 hr and 24-48 hr, respectively. Bars depict mean and  
 808 standard error for four cultures per treatment; double asterisks indicate that the treatment  
 809 mean was significantly different from the mean of positive control cultures (*bar f*) at  $p <$   
 810 0.01. *NS*, no significant difference ( $p > 0.05$ ) in the activation index.

811

812 Fig. 2. Dose-dependent effect of cation-channel inhibitors on stretch-activation of satellite  
 813 cells and up-stream HGF release. Panel *A*, satellite cells were subjected to an environment  
 814 of cyclic stretch for 1 hr beginning at 24-hr post-plating in the presence of various  
 815 concentrations of individual cation-channel inhibitors, GsMTx-4 (*closed circle*), nifedipine  
 816 (*closed square*), gadolinium chloride (*open circle*), and NNC55-0396 (*open square*), and  
 817 assayed for BrdU-incorporation at 48-hr post-plating. This experiment also included  
 818 control cultures as follows: *bar a*, un-stretched culture (*white bar*); *bar b*, 1-hr stretch  
 819 culture (*black bar* marked *Positive Control*); *bars c-g*, control cultures receiving 2.5 ng/ml  
 820 HGF at 24-48 hr post-plating along with none, 0.1  $\mu$ M GsMTx-4, 10  $\mu$ M nifedipine, 100  
 821  $\mu$ M gadolinium chloride, and 100  $\mu$ M NNC55-0396, respectively (*grayed bars*); *bars h-j*,  
 822 un-stretched cultures with individual cation-channel inhibitors (each at the optimal  
 823 concentration). Data points and bars depict mean and standard error of four cultures per  
 824 treatment; single and double asterisks indicate that the treatment mean was significantly  
 825 different from the mean of positive control cultures (*bar b*) at  $p < 0.05$  and  $p < 0.01$ ,  
 826 respectively. Panel *B*, a typical data set of ECL-western blotting of HGF in two or three

827 independent experiments; conditioned media (serum-free DMEM) from 1-hr stretch  
828 cultures with none (*lane m*), 0.1  $\mu$ M GsMTx-4 (*lane n*), 10  $\mu$ M nifedipine (*lane o*) or 1.8  
829 mM EGTA (*lane p*), were analyzed for HGF release from the extracellular tethering by  
830 ECL-western blotting standardized with internal  $\beta$ -actin in cell lysates that were harvested  
831 after stretch. *Lane q*, un-stretch medium; *k*, molecular weight standards (STD); *l*, mouse  
832 recombinant HGF (12 ng) to show the band at 60-kDa  $\alpha$ -chain for active HGF (*upper row*)  
833 and 42-kDa  $\beta$ -actin in mouse C2C12 myoblasts (*lower row*) as positive controls (PC); *r*,  
834 negative controls (NC) of stretch medium (*upper row*) and whole cell lysate (*lower row*)  
835 blotted without the primary antibody and with secondary antibody.

836

837 Fig. 3. Detection of mRNA for the L-type voltage-gated calcium channel  
838 (L-VGC-channel) and transient receptor potential canonical channels 1 and 6 (TRPC1, 6) in  
839 satellite cells. Satellite cell cultures were maintained in DMEM-10% HS and assayed for  
840 mRNA expression of  $\alpha_{1S}$ ,  $\alpha_{1C}$ ,  $\alpha_{1D}$ ,  $\alpha_{1F}$  subunits of the L-VGC-channel (panel *A*) and  
841 TRPC1, 6 (panel *B*) at 24-hr post-plating by RT-PCR. Bands were visualized with  
842 Gel-Red staining after agarose gel electrophoresis. *NC*, negative controls (satellite cell  
843 mRNA without reverse transcription); *SCs*, satellite cells; *PC*, positive controls (rat skeletal  
844 muscle for  $\alpha_{1S}$  and TRPC1, cardiac muscle for  $\alpha_{1C}$ , brain for  $\alpha_{1D}$  and TRPC6, and eye for  
845  $\alpha_{1F}$ ).

846

847 Fig. 4. Effect of cation-channel inhibitors and EGTA on the increase in intracellular  
848 calcium ion concentration in response to stretch. Calcium-imaging analysis was conducted  
849 under the StageFlexer Jr. system using Fluo3-loaded satellite cells that were treated with  
850 individual cation-channel inhibitors (0.1  $\mu$ M GsMTx-4, 10  $\mu$ M nifedipine) for 30-min just  
851 prior to adding two cycles of stretch at 24-hr post-plating. Row +*EGTA*, cells were  
852 incubated with 1.8 mM EGTA in DMEM-10% HS just prior to the addition of the stretch.  
853 Companion cells were treated with 3  $\mu$ M A23187 (a calcium ionophore) and served as a  
854 positive control (row *A23187*) (67). Fluorescence intensity was assigned from blue to red  
855 in color-coded images; the normal resting free calcium-ion level was represented by blue,  
856 and gradual increases were demonstrated by a change to yellow and then red. After  
857 calcium imaging, cells were visualized by immunostaining to confirm the presence of c-met,  
858 a marker molecule for myogenic cells in our primary cell cultures (DAB-stained images not  
859 shown).

860

861 Fig. 5. A possible mechanism of satellite cell activation in response to mechanical stimuli.

862 Panel *A*, reproduced from Fig. 4 of Tatsumi and Allen (66) with some modifications.

863 Ca-CaM, calcium-calmodulin complex; L-Arg, L-arginine; NOS, NO synthase; MMP2,

864 matrix metalloproteinase 2. Panel *B*, calcium ion influx mechanism was examined in the

865 present study and the model was schematically presented. Steps 1 and 2: cations stream

866 into the cell through mechano-sensitive cation channels (MS-channel) to induce local

867 depolarization of the cell membrane (changes in membrane potential); step 3: depolarization

868 promotes gating of adjacent L-type voltage-gated calcium-ion channels (L-VGC-channel),

869 and the result is calcium ion influx that promotes formation of the Ca-CaM complex that

870 initiates NOS activity.

871

872

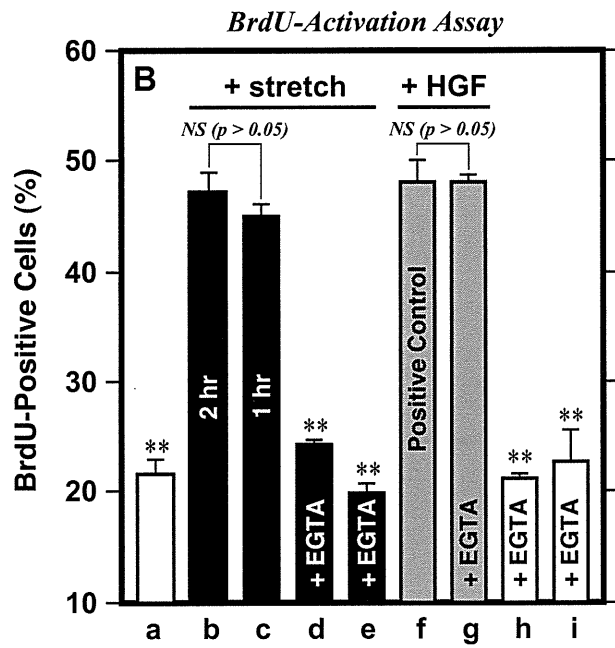
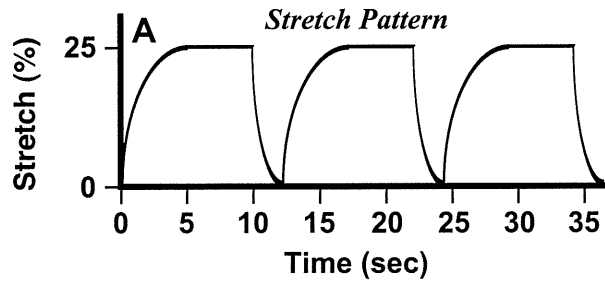


**Fig. 1, Hara et al.**

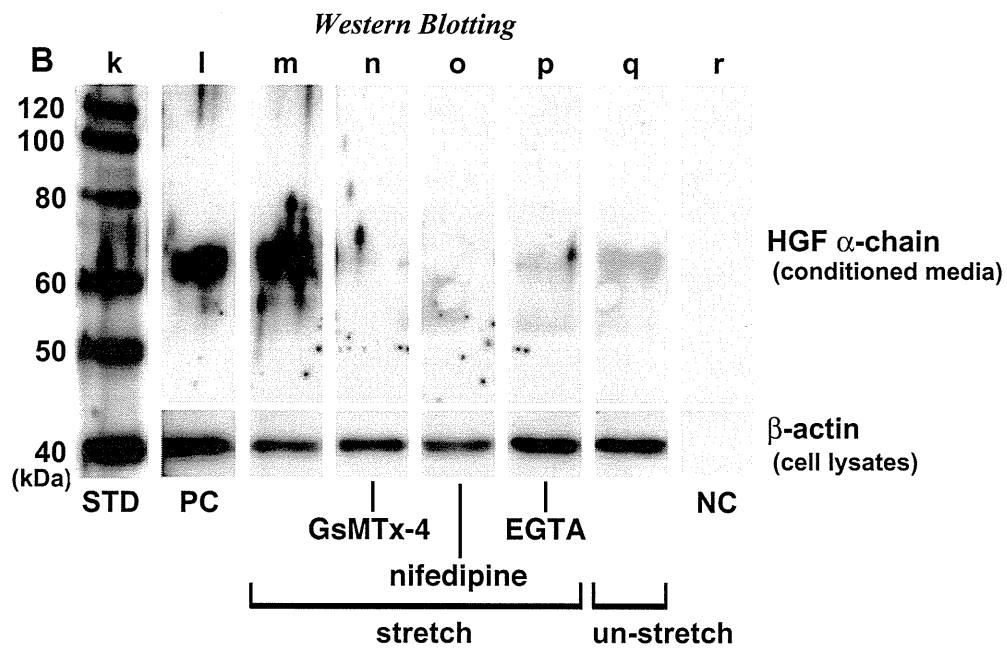
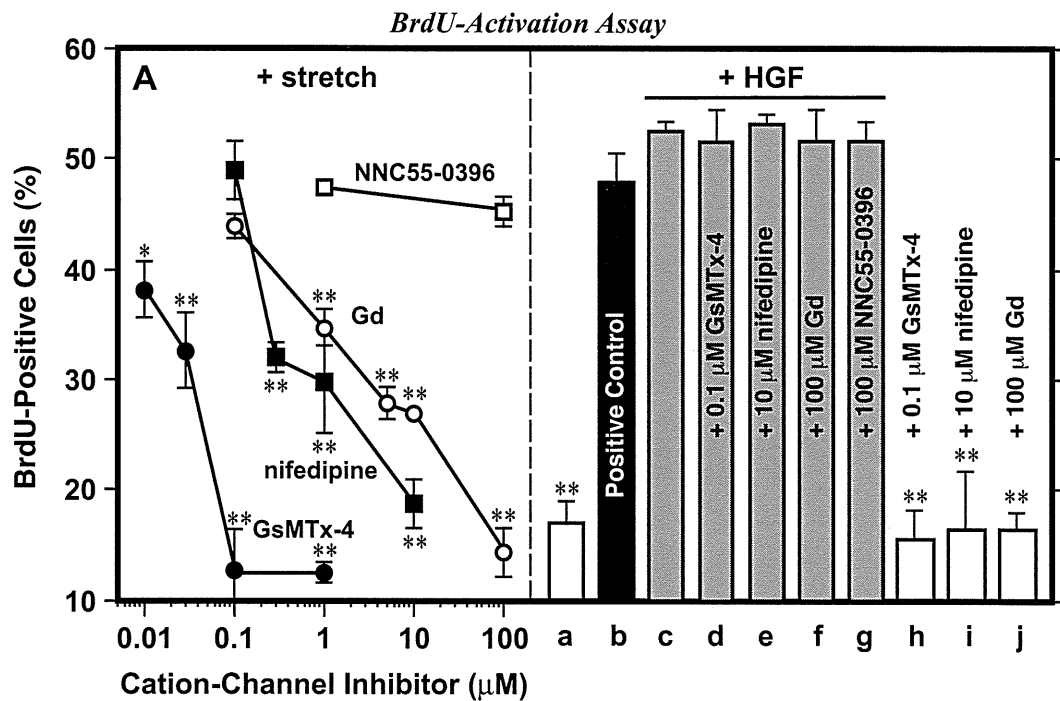


**Fig. 2, Hara et al.**

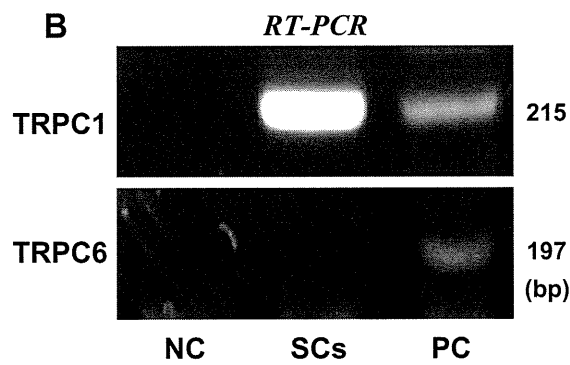
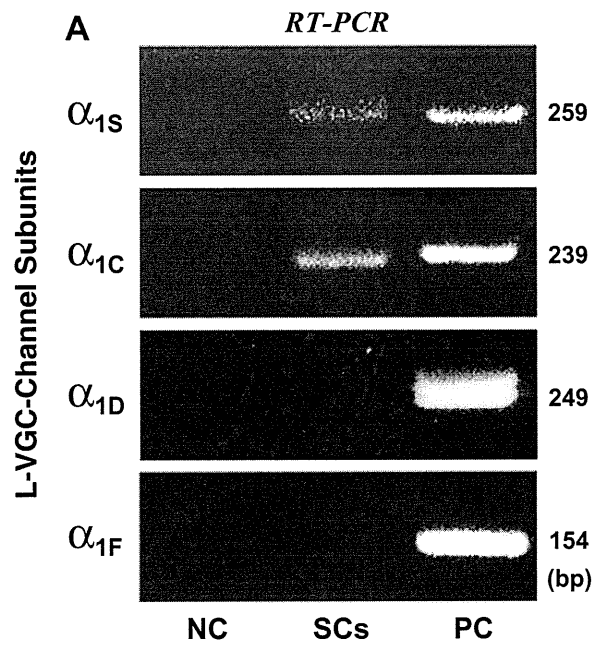


**Fig. 3, Hara *et al.***



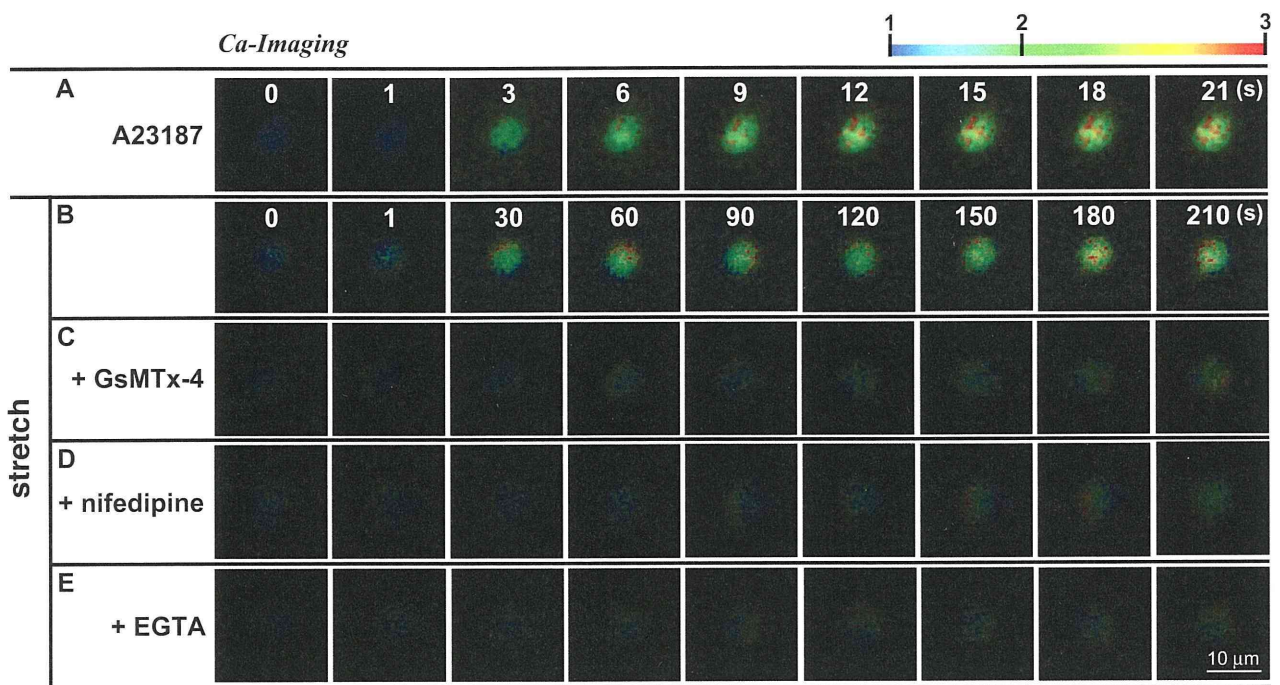


Fig. 4, Hara *et al.*

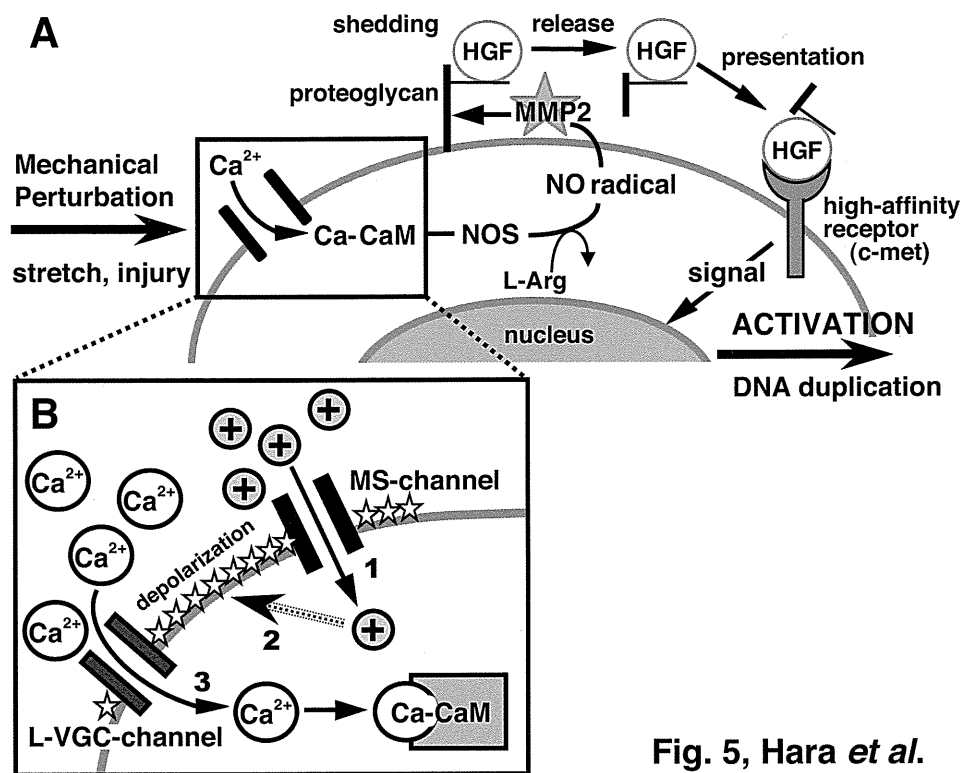


Fig. 5, Hara *et al.*

# Beraprost sodium, a stable prostacyclin analogue, improves insulin resistance in high-fat diet-induced obese mice

Eriko Inoue<sup>1</sup>, Toshihiro Ichiki<sup>1,2</sup>, Kotaro Takeda<sup>1,2</sup>, Hirohide Matsuura<sup>1</sup>, Toru Hashimoto<sup>1</sup>, Jiro Ikeda<sup>1</sup>, Aya Kamiharaguchi<sup>1</sup> and Kenji Sunagawa<sup>1</sup>

Departments of <sup>1</sup>Cardiovascular Medicine and <sup>2</sup>Advanced Therapeutics for Cardiovascular Diseases, Kyushu University Graduate School of Medical Sciences, Fukuoka, Japan

(Correspondence should be addressed to T Ichiki at Department of Advanced Therapeutics for Cardiovascular Diseases, Kyushu University Graduate School of Medical Sciences; Email: [ichiki@cardiol.med.kyushu-u.ac.jp](mailto:ichiki@cardiol.med.kyushu-u.ac.jp))

## Abstract

Obesity induces hypertrophy of adipocyte resulting in production of pro-inflammatory cytokines such as tumor necrosis factor- $\alpha$  (TNF- $\alpha$ ) and monocyte chemoattractant protein 1 (MCP1 (CCL2)). These cytokines play an important role in the development of insulin resistance. Beraprost sodium (BPS), a prostaglandin I<sub>2</sub> analogue, is reported to attenuate inflammation. In this study, we examined the effect of BPS on glucose metabolism in mice fed a high-fat diet (HFD). Four-week-old C57/B6 male mice were fed a HFD for 12 weeks (HFD group) and the treatment group received oral BPS (300  $\mu$ g/kg per day) for the same period. Then, glucose metabolism, histological changes, and gene expression of white adipose tissue (WAT) were examined. Body weight was increased, and glucose

intolerance and insulin resistance were developed in the HFD group. Treatment with BPS improved glucose tolerance and insulin action without body weight change. Histological analysis of WAT showed an increase in the size of adipocyte and macrophage infiltration in the HFD group, which was attenuated by BPS treatment. BPS reduced HFD-induced expression of MCP1 and TNF- $\alpha$  in WAT. BPS also attenuated hepatic steatosis induced by the HFD. These results suggest that BPS improved glucose intolerance possibly through suppression of inflammatory cytokines in WAT. BPS may be beneficial for the treatment of obesity-associated glucose intolerance.

*Journal of Endocrinology* (2012) **213**, 285–291

## Introduction

Obesity plays a central role in the development of metabolic syndrome (Wajchenberg 2000), a constellation of risk factors such as insulin resistance, dyslipidemia, and high blood pressure. Accumulation of visceral fat rather than subcutaneous fat is believed to cause insulin resistance (Wajchenberg 2000, Masuzaki *et al.* 2001). In obesity, adipocytes are enlarged and increased in number, and an excess of lipid leads to ectopic deposition of triglyceride in the liver and muscle, which is one of the causes of insulin resistance (Savage *et al.* 2007). The hypertrophied adipocytes produce proinflammatory cytokines such as monocyte chemoattractant protein-1 (MCP1 (CCL2)) and tumor necrosis factor- $\alpha$  (TNF- $\alpha$ ) as obesity progresses (Shoelson *et al.* 2006). These cytokines, so-called adipokines, cause inflammation and recruitment of macrophages to adipose tissue (Xu *et al.* 2003), which is another important mechanism for obesity-induced insulin resistance. The infiltrated macrophages enhance inflammation of adipose tissue, indicating that these processes form a vicious circle.

TNF- $\alpha$  induces c-Jun amino-terminal kinase (JNK) activation and phosphorylation of insulin receptor substrate 1 (IRS1) at serine residues that negatively regulate normal signaling through the insulin receptor/IRS1 axis (Hotamisligil *et al.* 1996). Mice lacking chemokine receptor-2 (CCR2), a receptor for MCP1, are partly protected against developing high-fat diet (HFD)-induced insulin resistance and exhibit reductions in adipose tissue macrophage recruitment and inflammatory gene expression (Weisberg *et al.* 2006). These observations suggest that adipose tissue in obesity is characterized by chronic low-grade inflammation, and inflammatory cytokines play a causative role in the development of insulin resistance.

Beraprost sodium (BPS) is a stable prostaglandin I<sub>2</sub> analogue and has a potent vasodilating effect through activation of prostacyclin receptor (Olschewski *et al.* 2004). BPS is also reported to attenuate inflammation. BPS reduced serum TNF- $\alpha$  levels in diabetic patients (Fujiwara *et al.* 2004) and expression of *Mcp1* mRNA in the kidney of Otsuka Long-Evans Tokushima fatty (OLETF) rats, resulting in the amelioration of diabetic nephropathy (Watanabe *et al.* 2009). BPS inhibits

TNF- $\alpha$ -induced expression of vascular cell adhesion molecule and monocyte attachment to endothelial cells (Goya *et al.* 2003). We therefore hypothesized that the anti-inflammatory effects of BPS may be beneficial for the improvement of obesity-induced insulin resistance, in which inflammation plays an important role.

We showed in this study that BPS improved glucose metabolism in association with reduction of inflammation of white adipose tissue (WAT) in a mouse model of diet-induced obesity.

## Materials and Methods

### Animals

All procedures were approved by the institutional animal use and care committee and were conducted in conformity with institutional guidelines. Four-week-old C57/B6 mice were purchased from Kyudo Co. Ltd. (Tosu, Saga, Japan). Three groups were analyzed: mice fed a normal chow diet (control group), mice fed a HFD containing 60% kcal fat (High Fat Diet 32, Clea Japan (Tokyo); HFD group) for 12 weeks, and mice fed a HFD and administered BPS for 12 weeks (BPS group). BPS dissolved in water at 1.5  $\mu\text{g}/\text{ml}$  was given *ad libitum* because of the short half-life of BPS ( $\sim 1$  h). As a preliminary study showed that the estimated volume of water intake was  $\sim 0.2$  ml/g per day, the estimated dose of orally ingested BPS was 300  $\mu\text{g}/\text{kg}$  per day. At the end of the experiment, systolic blood pressure (SBP) and heart rate (HR) were measured by a tail-cuff method (BP-98A, Softron Co., Tokyo, Japan). Mice were killed by CO<sub>2</sub> inhalation.

### Histological analysis

Adipose tissues were fixed with 10% formaldehyde for 24 h. The specimens were embedded into paraffin. Paraffin sections were stained with hematoxylin and eosin (H&E). The cross-sectional area for each adipocyte was determined using Dynamic cell count BZ-HIC (Keyence, Osaka, Japan). To detect macrophage infiltration, the paraffin sections were stained with an antimouse MAC3 (LAMP2) antibody (Santa Cruz Biotechnology, Inc., Santa Cruz, CA, USA). Sections were deparaffinized with xylene and refixed with ethanol for 40 min, immersed in PBS, and then autoclaved in citrate buffer for antigen retrieval. Then, the sections were incubated with 3% hydrogen peroxide in methanol for 20 min. The sections were further incubated with an antibody against MAC3 (1:200) overnight at 4 °C. After rinsing with PBS, the sections were incubated with biotin-labeled goat anti-rabbit IgG antiserum (Santa Cruz Biotechnology, Inc., 1:200 dilution) for 30 min and then incubated with avidin-biotin complex (Vectastain ABC kit; 1:100 dilution) for 15 min, and the sections were incubated with 3,3'-diaminobenzidine and 0.03% hydrogen peroxide in deionized water for about 80 s. The number of MAC3-positive cell clusters was counted in high power field (HPF). The data are mean of five randomly chosen HPFs. After the mice were killed, the livers were removed and subsequently fixed in 10% formaldehyde. The sections were embedded in

paraffin blocks and stained with H&E to examine the structures of the liver and evaluate lipid droplets. For the quantification of areas of lipid accumulation in the liver, H&E-stained images of liver were uploaded into a computer for analysis. The images were processed into two gradations (black and white). The white porosity areas were quantified as vacuolation (Sato *et al.* 2010), which mostly represents accumulation of lipid droplets. Contribution of arteries, veins, and bile ducts to porosity area was small and equally observed in the three groups and therefore ignored in the quantification. The data are expressed as a percentage of white area to total area.

### Glucose tolerance test and insulin tolerance test

Mice were starved for 6 h. Then, the mice were i.p. injected with glucose (1 g/kg of body weight) for the glucose tolerance test (GTT). For the insulin tolerance test (ITT), the mice were i.p. injected with rapid insulin (0.5 IU/kg of body weight). Blood was taken from tail vein at various time points to measure blood glucose concentrations by Glutest Every (Sanwa Kagaku Kenkyusho, Nagoya, Japan).

### Measurement of serum levels of triglyceride, cholesterol, and insulin

Serum triglyceride and total cholesterol levels were determined by commercially available kits, Triglyceride E-test Wako (Wako, Osaka, Japan) and Cholesterol E-test Wako (Wako) respectively. Serum insulin levels were determined by ELISA kit (Morinaga Institute of Biological Science, Yokohama, Japan).

### RNA extraction and real-time quantitative RT-PCR analysis

RNA from adipose tissue was extracted using ISOGEN according to the manufacturer's instruction (Wako). One microgram of total RNA was reverse transcribed using ReverTra Ace qPCR RT Kit (Toyobo, Osaka, Japan). Real-time quantitative PCR (qPCR) was performed using 7500 real-time PCR system (Applied Biosystems) and SYBER Green PCR Master Mix (Applied Biosystems). Primer sequences for real-time qPCR used in this study are as follows:

TNF- $\alpha$ : 5'-AAGCCTGTAGCCCACGTCGTA-3';  
5'-GGCACCACACTAGTTGGTTGTCTTTG-3'.  
MCP1: 5'-TTAACGCCCCACTCACCTGCTG-3';  
5'-GCTTCTTTGGGACACCTGCTGC-3'.  
PPAR $\gamma$  (PPARG):  
5'-TGTCGGTTTCAGAAGTGCCTTG-3';  
5'-TTCAGCTGGTTCGATATCACTGGAG-3'.  
C/EBP $\alpha$ : 5'-TTGAAGCACAATCGATCCATCC-3';  
5'-GCACACTGCCATTGCACAAG-3'.  
Adiponectin: 5'-GTCAGTGGATCTGACGACACCAA-3';  
5'-ATGCCTGCCATCCAACCTG-3'.  
18S rRNA: 5'-ACTCAACACGGGAAACCTCA-3';  
5'-AACCAGACAAATCGCTCCAC-3'.